Journal of Alloys and Compounds 506 (2010) 302–307

Contents lists available at ScienceDirect

Journal of Alloys and Compounds

journal homepage: www.elsevier.com/locate/jallcom

Crystallization kinetics of $Mg_{61}Cu_{28}Gd_{11}$ and $(Mg_{61}Cu_{28}Gd_{11})_{99.5}Sb_{0.5}$ bulk metallic glasses

Y.D. Sun, Z.Q. Li*, J.S. Liu, J.N. Yang, M.Q. Cong

College of Materials Science and Technology, Nanjing University of Aeronautics and Astronautics, NO. 29 Yudao Street, Nanjing 210016, China

ARTICLE INFO

Article history:
Received 5 May 2010
Received in revised form 29 June 2010
Accepted 30 June 2010
Available online 7 July 2010

Keywords:
Amorphous alloys
Thermal analysis
Crystallization kinetics

ABSTRACT

The crystallization behavior of $Mg_{61}Cu_{28}Gd_{11}$ and $(Mg_{61}Cu_{28}Gd_{11})_{99.5}Sb_{0.5}$ bulk metallic glasses was studied using differential scanning calorimeter technique under different heating conditions. Under isochronal heating, the onset and peak temperatures of crystallization for these glasses exhibit strong heating-rate dependence. The activation energies for onset and peak crystallization were determined, based on Kissinger plots, to be 77 and 79 kJ/mol, respectively, for $Mg_{61}Cu_{28}Gd_{11}$ glassy alloy, and 104 and 108 kJ/mol, respectively, for $(Mg_{61}Cu_{28}Gd_{11})_{99.5}Sb_{0.5}$ glassy alloy. The isothermal kinetics was modeled by the Johnson–Mehl–Avrami equation. The Avrami exponents suggest that the isothermal crystallizations of the two glassy alloys are both governed by diffusion-controlled growth. On the basis of Arrhenius relation, the activation energies in the isothermal process were calculated to be 88 and 112 kJ/mol, respectively for $Mg_{61}Cu_{28}Gd_{11}$ and $(Mg_{61}Cu_{28}Gd_{11})_{99.5}Sb_{0.5}$ glassy alloys. The superior thermal stability of Sb-additive glassy alloy can be attributed to the strong affinity for Sb/Mg and Sb/Gd, which appears to impose resistance to the formation of Mg_2Cu and Cu_5Gd phases.

1. Introduction

Mg-based bulk metallic glasses (BMGs) have attracted increasing interests in recent years due to their high specific strength and relatively low cost [1–4]. Among them, the Mg–Cu–Gd ternary system exhibits superior glass forming ability as compared with Mg–Cu–Y and Mg–Ni–Y systems, and has become the active research area in Mg-based BMGs [5–7]. The fracture strength of Mg–Cu–Gd-based BMGs has been reported to achieve 900–1005 MPa, which is about twice as high as the highest strength for conventional Mg-based crystalline alloys [8–11]. As promising engineering materials, the thermal stability (i.e. crystallization resistance) of BMGs is also considered as one of the greatest important aspects for the application, and thus the crystallization behavior with the increasing temperature could be the critical point of understanding the mechanisms of phase transformation far from equilibrium [12–14]. In general, it is the differential scanning calorimetry (DSC) technique that is used to investigate isochronal and isothermal crystallization processes and analyze the crystallization kinetics of glassy alloys, as has been confirmed in Zr- [15–17], Pd- [18], Mg- [19–21], Ti- [22] and Fe-based [23–25] glassy alloys.

To date, the addition of quaternary element is an effective method to improve the thermal stability of Mg–Cu–RE (RE = Y, Gd) glassy alloy. Cheng et al. [19] have studied the effect of B addition on thermal stability and crystallization kinetics of $Mg_{65}Cu_{25}Y_{10}$ glassy alloy, and confirmed that the minor B element appears to enhance the thermal stability of Mg–Cu–Y–B alloy. Chang et al. [20] have investigated the crystallization processes of $Mg_{65}Cu_{25}Gd_{10}$ glassy alloy with Ag addition. It has been found that the activation energy of crystallization is increased by minor addition of Ag, and the main crystallization process for $Mg_{65}Cu_{22.5}Gd_{10}Ag_{2.5}$ glassy alloy is governed by diffusion controlled crystal growth with decreasing nucleation rate [20]. As can be seen, both the B and Ag elements have negative heat of mixing, ΔH_m (for liquid phase), with the main constitutes of Mg–Cu–Y/Gd glassy alloys [26]. However, the elements that exhibit partial positive ΔH_m with main constitutes have not been reported to improve the thermal stability of Mg–Cu–Gd glassy alloy, such as Sb (Cu–Sb: +7 kJ/mol) [26].

This work aims to investigate the crystallization kinetics of $Mg_{61}Cu_{28}Gd_{11}$ and $(Mg_{61}Cu_{28}Gd_{11})_{99.5}Sb_{0.5}$ BMGs. The isochronal and isothermal DSC annealing techniques are employed to investigate the crystallization behaviors of two glassy alloys. The details of the nucleation and growth behaviors in the crystallization process are explained by the parameters of activation energy and Avrami exponent. The effect of minor addition Sb on thermal stability of Mg–Cu–Gd glassy alloy is also discussed in this paper.

2. Experimental

Elements with purity better than 99.9% were used as starting materials. Cu–Gd as intermediate alloy was melted prior to be re-melted with Mg and Sb to obtain the master alloy. The glasses were prepared by copper mold casting with a diameter of 2 mm and a length of 50 mm.

* Corresponding author. Tel.: +86 25 5211 2913; fax: +86 25 52112626.
E-mail addresses: ziquanli@hotmail.com, ziquanli@nuaa.edu.cn (Z.Q. Li).

0925-8388/$ – see front matter © 2010 Elsevier B.V. All rights reserved.
doi:10.1016/j.jallcom.2010.06.196

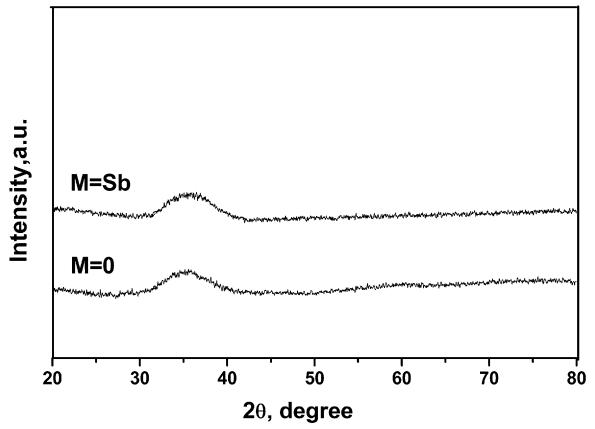

Fig. 1. XRD patterns of as-prepared $(Mg_{61}Cu_{28}Gd_{11})_{99.5}M_{0.5}$ (M = 0, Sb) BMGs.

The structures of the samples obtained were examined by X-ray diffraction (XRD, Bruker D8) with Cu Kα radiation. The crystallization process of the $Mg_{61}Cu_{28}Gd_{11}$ and $(Mg_{61}Cu_{28}Gd_{11})_{99.5}Sb_{0.5}$ amorphous alloys was characterized by continuous heating and isothermal annealing in a DSC (Perkin-Elmer DSC 7) under flowing high purity argon. In the case of continuous heating, the DSC plots were recorded at heating rates of 10–80 K/min. For the isothermal analysis, the amorphous samples were firstly heated at a rate of 50 K/min to a fixed temperature (between 464 and 479 K), and then held for a certain period of time until completion of crystallization. It should be mentioned that the possible temperature values at the beginning of the isothermal measurement are usually 5 K lower than the fixed temperatures due to the temperature lag effect. Al_2O_3 and Al pans were utilized for the continuous heating and the isothermal annealing, respectively. The DSC system was calibrated for temperature and enthalpy by using zinc and indium standards, giving an accuracy of ±0.2 K and ±0.02 mW, respectively. For each test sample, two identical DSC runs were carried out. The second run was served as in situ recorded with the baseline. This baseline was then subtracted by the first run DSC to count the correction for the apparatus baseline shift. It should be noted that to acquire the better accuracy in the DSC measurements, the test weight of each sample was at least 5 mg.

The $Mg_{61}Cu_{28}Gd_{11}$ and $(Mg_{61}Cu_{28}Gd_{11})_{99.5}Sb_{0.5}$ glassy samples were annealed isothermally at 469 K for 20 min and the annealed samples were investigated by X-ray diffraction with Cu Kα radiation to verify the phases formed upon crystallization.

3. Results and discussion

Fig. 1 shows the XRD patterns of as-prepared $Mg_{61}Cu_{28}Gd_{11}$ and $(Mg_{61}Cu_{28}Gd_{11})_{99.5}Sb_{0.5}$ samples. The alloys both exhibit an XRD pattern typical for the amorphous phase without an obvious crystalline peak.

Fig. 2 shows the DSC curves of $Mg_{61}Cu_{28}Gd_{11}$ (a) and $(Mg_{61}Cu_{28}Gd_{11})_{99.5}Sb_{0.5}$ (b) glassy alloys obtained at various heating rates of 10, 20, 30, 40 and 80 K/min. The values of glass transition temperature T_g, onset temperature of crystallization T_x, peak temperature T_p and ΔT_x (defined as temperature region between T_g and T_x), as well as the exothermic enthalpy ΔH_x at different heating rates are listed in Table 1. It is clearly seen that T_g, T_x and T_p, shift to higher temperatures with the increasing heating rate. The crystallization of samples is rate dependent caused by the fact that nucleation is a thermally activated process, whereas the rate dependence of the kinetic glass transition is due to the relaxation processes in the glass transition region [27]. This phenomenon has been also reported for Zr-based BMGs [28].

The effective activation energy of crystallization processes can be calculated by means of the Kissinger equation [29]:

$$\ln\left(\frac{\phi}{T^2}\right) = -\frac{E}{RT} + C \quad (1)$$

where ϕ is the heating rate, R is the gas constant, T represents the specific temperature, such as T_x or T_p, and C is a constant. By plotting $\ln(\phi/T^2)$ vs. $1/T$, an approximately straight line with a slope of E_x and E_p can be obtained, as shown in Fig. 3, in which E_x and

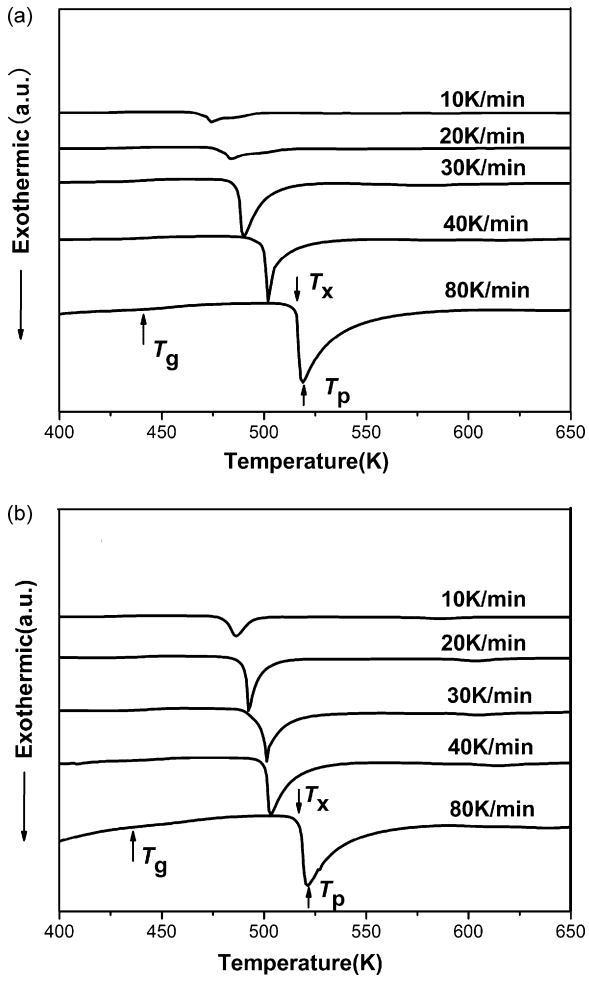

Fig. 2. Continuous heating DSC curves of amorphous $Mg_{61}Cu_{28}Gd_{11}$ (a) and $(Mg_{61}Cu_{28}Gd_{11})_{99.5}Sb_{0.5}$ (b) alloys at different heating rates of 10, 20, 30, 40 and 80 K/min.

E_p are the effective activation energy for the onset and peak temperature of crystallization. From the slope of the straight lines, we derived the values of activation energy and obtained E_x = 77 kJ/mol (±9 kJ/mol), E_p = 79 kJ/mol (±10 kJ/mol) for $Mg_{61}Cu_{28}Gd_{11}$ alloy, and E_x = 104 kJ/mol (±9 kJ/mol), E_p = 108 kJ/mol (±8 kJ/mol) for $(Mg_{61}Cu_{28}Gd_{11})_{99.5}Sb_{0.5}$ alloy. The Sb-additive alloy exhibits the E_x and E_p about 35% higher than the parent alloy, suggesting the larger energy barriers of onset and peak crystallization for $(Mg_{61}Cu_{28}Gd_{11})_{99.5}Sb_{0.5}$ glassy alloy. Accordingly, the resistance ability to crystallization as well as the thermal stability has been

Table 1
The characteristic temperatures T_g, T_x, T_p, ΔT_x and ΔH_x of $Mg_{61}Cu_{28}Gd_{11}$ (a) and $(Mg_{61}Cu_{28}Gd_{11})_{99.5}Sb_{0.5}$ (b) glassy alloys at different heating rates.

Heating rate (K/min)	T_g (K) (±1)	T_x (K) (±1)	T_p (K) (±1)	ΔT_x (K)	ΔH_x (J/g) (±2)
(a)					
10	415	471	474	56	51
20	419	480	483	61	54
30	423	488	490	65	56
40	429	500	502	71	56
80	440	517	520	77	60
(b)					
10	417	480	486	63	54
20	422	490	492	68	56
30	424	495	501	71	58
40	427	502	503	75	60
80	436	518	522	82	63

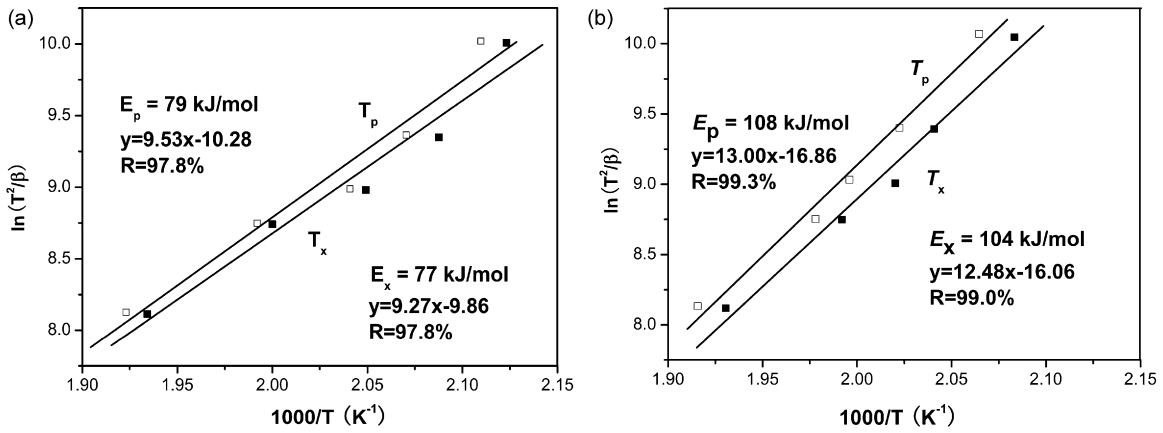

Fig. 3. The Kissinger plots for onset and peak temperatures of crystallization for $Mg_{61}Cu_{28}Gd_{11}$ (a) and $(Mg_{61}Cu_{28}Gd_{11})_{99.5}Sb_{0.5}$ (b) BMGs.

improved by the Sb addition. In addition, the E_p values of the two glassy alloys are both higher than their E_x values. It is generally known that the onset temperature of crystallization associates with the nucleation process, and the peak temperature is related to the growth process. It may presume that the activation energies deduced from onset and peak temperatures of crystallization represent the activation energy for nucleation and growth, respectively [30,31]. Therefore, for the two glassy alloys, the fact that the E_x values deduced from Kissinger's method are lower than the E_p values means the nucleation process is easier than growth one.

Their isothermal kinetics of crystallization was further studied with DSC at annealing temperatures of 464, 469, 474 and 479 K, and the corresponding DSC plots are shown in Fig. 4. Similar to continuous heating, all DSC traces exhibit a single exothermic peak after passing a certain incubation period and the incubation time (τ) as well as the exothermic enthalpy ΔH_x at different temperatures is shown in Table 2. From the table, it is clear that the incubation time τ (defined as the time interval between the specimens reaching the annealing temperature and the start of the transformation) becomes shorter when the annealing temperature is higher for both the glassy alloys. These facts indicate that the amorphous phase crystallizes via a nucleation-and-growth process [32]. Moreover, as the annealing temperature decreases, the exothermic peak width (referred to the time between 1 and 95% of transformation into the

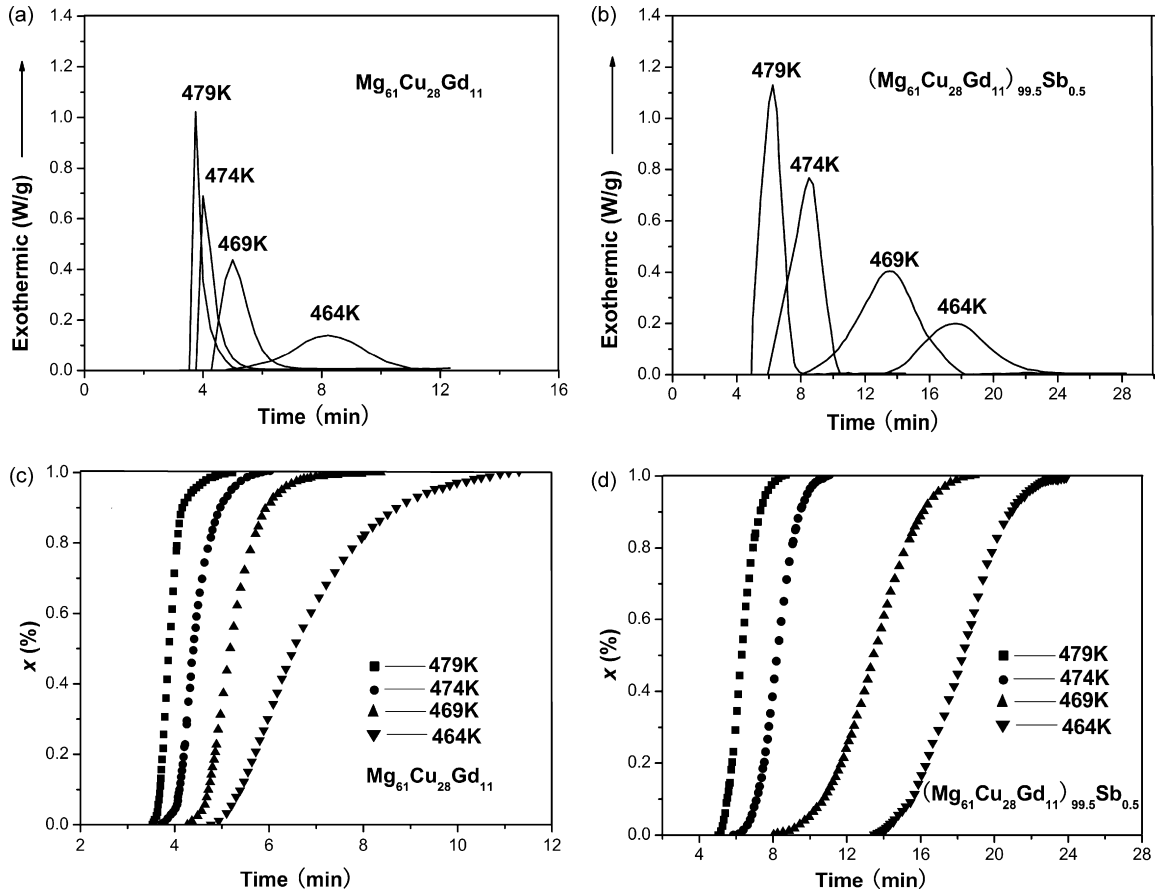

Fig. 4. Isothermal DSC curves and the crystallized volume fraction as a function of annealing time for $Mg_{61}Cu_{28}Gd_{11}$ (a and c) and $(Mg_{61}Cu_{28}Gd_{11})_{99.5}Sb_{0.5}$ (b and d) glassy alloys at different annealing temperatures.

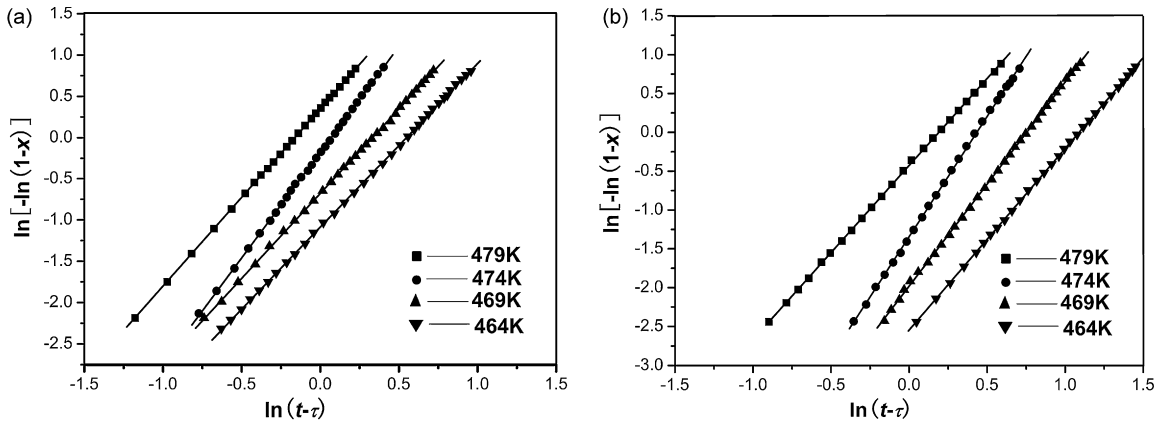

Fig. 5. The JMA plots for the isothermal crystallization of $Mg_{61}Cu_{28}Gd_{11}$ (a) and $(Mg_{61}Cu_{28}Gd_{11})_{99.5}Sb_{0.5}$ (b) glassy alloys at different annealing temperatures.

Table 2
The kinetic parameters and ΔH_x of $Mg_{61}Cu_{28}Gd_{11}$ (a) and $(Mg_{61}Cu_{28}Gd_{11})_{99.5}Sb_{0.5}$ (b) glassy alloys in the case of isothermal annealing.

Annealing temperature (K)	Incubation time, τ (min) (±0.25)	Avrami exponent, n (±0.01)	Reaction constant, k (±0.001)	ΔH_x (J/g) (±2)
(a)				
464	4.84	1.98	0.577	54
469	4.29	2.06	0.719	54
474	3.76	2.56	0.932	57
479	3.52	2.15	1.174	60
(b)				
464	12.94	2.34	0.336	65
469	8.05	2.63	0.472	68
474	5.98	3.09	0.651	70
479	4.91	2.24	0.827	71

crystalline state) increases considerably, indicating a more sluggish crystallization process. Furthermore, as compared with the parent alloy, the Sb-additive alloy exhibits longer incubation time, indicating its retarded crystallization process.

It has been proposed that the fraction transformed x, up to any time t, is taken as proportional to the area of the exothermic peak, so the crystallized volume fraction during crystallization procedure can be accurately determined by measuring the partial area of the exothermic peak. The measurement results of $Mg_{61}Cu_{28}Gd_{11}$ and $(Mg_{61}Cu_{28}Gd_{11})_{99.5}Sb_{0.5}$ BMGs at different temperatures are shown in Fig. 4(c) and (d), respectively, which are of the usual sigmoid type. The isothermal phase transformation is usually modeled by the Johnson–Mehl–Avrami (JMA) equation [33–36]:

$$x(t) = 1 - \exp\{-[k(t-\tau)]\} \quad (2)$$

in which $x(t)$ is the crystallized volume fraction, t is the annealing time, n is the Avrami exponent, a constant related to the behavior of nucleation and growth, and k is a reaction rate constant which is function of annealing temperature and can be described by Arrhenius equation:

$$k = k_0 \exp\left[-\frac{E_c}{RT}\right] \quad (3)$$

Here k_0 is a constant and E_c is the apparent activation energy for crystallization. The values of k and n can be determined using the relationship:

$$\ln[-\ln(1-x)] = n \ln k + n \ln(t-\tau) \quad (4)$$

Plotting $\ln[-\ln(1-x)]$ vs. $\ln(t-\tau)$ at different annealing temperatures for the data x = 10–90%, the corresponding JMA plots of the two glassy alloys can be obtained and the results are shown in Fig. 5. The plots are nearly straight lines. The Avrami exponent n and the reaction constant k could be calculated from the slope and intercept of the straight line in Fig. 5 and the detailed results are shown in Table 2. It should be noted that the different values of Avrami exponents reflect the change in nucleation and growth behaviors in the process of crystallization. The Avrami exponents n are about 1.98–2.56 for $Mg_{61}Cu_{28}Gd_{11}$ alloy, and about 2.24–3.09 for $(Mg_{61}Cu_{28}Gd_{11})_{99.5}Sb_{0.5}$ alloy, which indicates that the growths

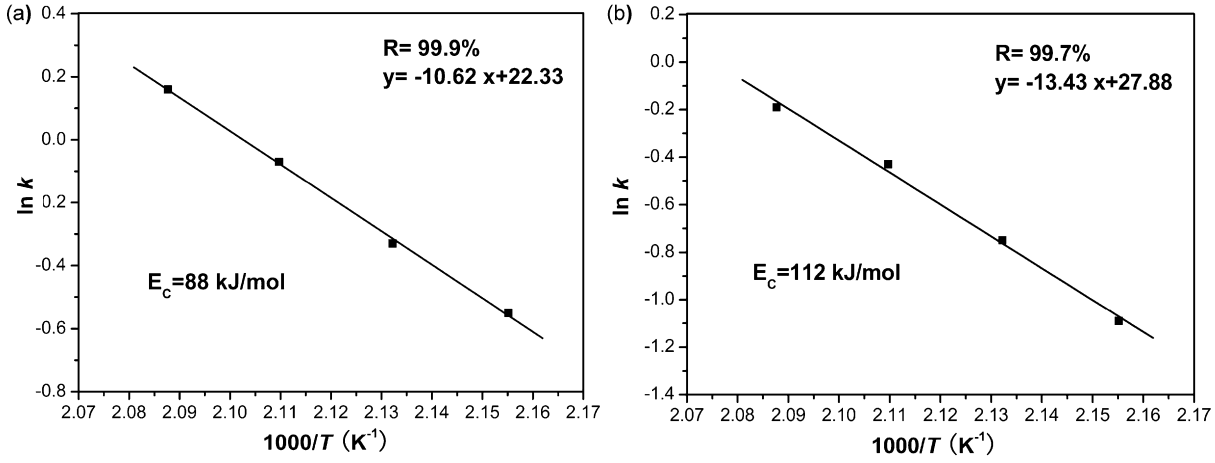

Fig. 6. Plots of the Arrhenious equation for the isothermal crystallization of $Mg_{61}Cu_{28}Gd_{11}$ (a) and $(Mg_{61}Cu_{28}Gd_{11})_{99.5}Sb_{0.5}$ (b), from which the activation energy of isothermal crystallization is obtained.

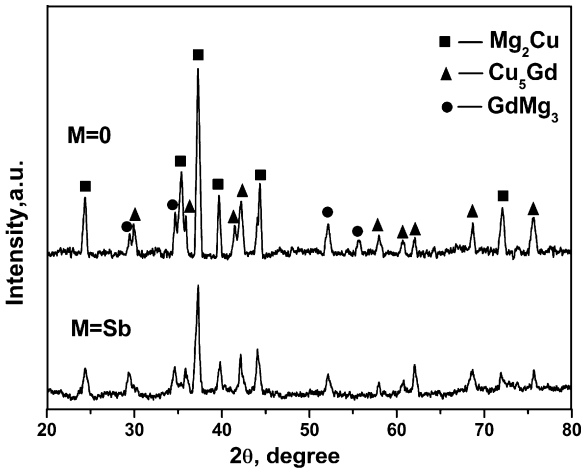

Fig. 7. XRD patterns of $(Mg_{61}Cu_{28}Gd_{11})_{99.5}M_{0.5}$ (M = 0, Sb) BMGs after isothermal annealing at 469 K for 20 min.

of the two glassy alloys are both diffusion-controlled [37]. Moreover, the variation of n values of the two glassy alloys indicates the crystallization mechanism changes from 464 to 479 K. At 464 K, the crystallizations of the two alloys are basically governed by a decreasing nucleation rate with time. Subsequently, the *n* values of $Mg_{61}Cu_{28}Gd_{11}$ and $(Mg_{61}Cu_{28}Gd_{11})_{99.5}Sb_{0.5}$ alloys increase to 2.56 and 2.63 at 474 K and 469 K, respectively, indicating an increasing nucleation rate. For the Sb-additive alloy, the *n* value achieves at 3.09 under the temperature of 474 K, implying the growth of the glassy alloy is still with the increasing nucleation rate. However, with the further increase of annealing temperature, the n values begin to decrease to be 2.15 and 2.24 for $Mg_{61}Cu_{28}Gd_{11}$ and $(Mg_{61}Cu_{28}Gd_{11})_{99.5}Sb_{0.5}$ BMGs, respectively, which both indicate the decreasing nucleation rate [37]. The variation of Avrami exponents can be attributed to the atomic diffusion in the alloy. The difficult atomic diffusion at low temperatures (such as 464 and 469 K) retards the nucleation and growth, resulting in a decreasing nucleation rate. With the further increase of temperature (up to 474 K), the atoms move relative easily in the supercooled liquid, this results in the increase of n values. However, at higher temperature (479 K), both the incubation time and the crystallization time become much shorter than those of lower temperature as shown in Table 2, so there is not enough time for the alloy to process the time-dependent nucleation and incubate large amount of new nuclei. This renders a possible explanation for the decreasing nucleation rate of crystallization at higher temperature.

Fig. 6 shows the plots of ln*k* vs. 1/*T* of $Mg_{61}Cu_{28}Gd_{11}$ (a) and $(Mg_{61}Cu_{28}Gd_{11})_{99.5}Sb_{0.5}$ (b) BMGs, which also yield a straight line. According to Eq. (3), the apparent activation energy for crystallization is calculated to be E_c = 88 kJ/mol (±2 kJ/mol) and E_c = 112 kJ/mol (±5 kJ/mol), respectively for the $Mg_{61}Cu_{28}Gd_{11}$ and $(Mg_{61}Cu_{28}Gd_{11})_{99.5}Sb_{0.5}$ alloys. These values are close to the ones derived from the Kissinger method, demonstrating that the crystallization on both isochronal and isothermal annealing follows a similar phase transformation mechanism.

To study the crystalline phases formed during the crystallization process, we annealed the $Mg_{61}Cu_{28}Gd_{11}$ and $(Mg_{61}Cu_{28}Gd_{11})_{99.5}Sb_{0.5}$ glassy samples isothermally at 469 K for 20 min. Fig. 7 shows the XRD patterns of the annealed samples, which are typical for all the samples of the two glassy alloys annealed to complete transformation. From these patterns, it is known that Mg_2Cu, Cu_5Gd and $GdMg_3$ are the major crystalline phases after the isothermal annealing treatment for $Mg_{61}Cu_{28}Gd_{11}$ and $(Mg_{61}Cu_{28}Gd_{11})_{99.5}Sb_{0.5}$ glassy alloys. It can be seen that the peak of Mg_2Cu and Cu_5Gd crystalline phases are apparently reduced with minor addition of Sb, implying that the atomic diffusion in Sb-additive alloy is more difficult comparing to the Sb-free alloy. This might be a result of multiple factors, including the larger overall atomic size difference, the increment of packing density in supercooled liquid and the higher overall electronegativity difference. Moreover, the strong affinity for Sb/Mg (ΔH_m = −16 kJ/mol) and Sb/Gd (ΔH_m = −68 kJ/mol) [26], together with the repulsion for Sb/Cu (ΔH_m = +7 kJ/mol) will impose resistance to the formation of the major Mg_2Cu and Cu_5Gd phase, possibly by blocking the path of Mg and Cu diffusion, and indirectly increase the crystallization energy barrier.

4. Conclusions

The crystallization kinetics of $Mg_{61}Cu_{28}Gd_{11}$ and $(Mg_{61}Cu_{28}Gd_{11})_{99.5}Sb_{0.5}$ BMGs were studied under different heating conditions. The isochronal and isothermal activation energies are both enhanced by minor addition of Sb. The isothermal kinetics was modeled by the JMA equation and the Avrami exponent indicates that the crystallizations of two alloys are both governed by diffusion-controlled growth. At 464 K, the $Mg_{61}Cu_{28}Gd_{11}$ and $(Mg_{61}Cu_{28}Gd_{11})_{99.5}Sb_{0.5}$ glassy alloys are both with the decreasing nucleation rate. With increase of temperature, the growth of nuclei changes to be with increasing nucleation rate. However, at higher temperature of 479K, the shortened incubation time, which is not enough for the time-dependent nucleation to incubate large amount of new nuclei results in the decrease of Avrami exponent. The superior thermal stability of Sb-additive glassy alloy can be attributed to the strong affinity for Sb/Mg and Sb/Gd, which appears to impose resistance to the formation of major Mg_2Cu and Cu_5Gd phases.

References

[1] C.M. Zhang, X. Hui, Z.G. Li, G.L. Chen, J. Alloys Compd. 467 (2009) 241–245.
[2] Y.L. Ren, R.L. Zhu, J. Sun, J.H. You, K.Q. Qiu, J. Alloys Compd. 493 (2010) L42–L46.
[3] J. Soubeyroux, S. Puech, J. Alloys Compd. 495 (2010) 330–333.
[4] Y. Sun, H.F. Zhang, H.M. Fu, A.M. Wang, Z.Q. Hu, Mater. Sci. Eng. A 502 (2009) 148–152.
[5] Q. Zheng, S. Cheng, J.H. Strader, E. Ma, J. Xu, Scripta Mater. 56 (2007) 161–164.
[6] V. Rangelova, T. Spassov, J. Alloys Compd. 345 (2002) 148–154.
[7] G.T. Bae, S.B. Lee, N.J. Kim, Mater. Sci. Eng. A 449–451 (2007) 489–492.
[8] D.G. Pan, W.Y. Liu, H.F. Zhang, A.M. Wang, Z.Q. Hu, J. Alloys Compd. 438 (2007) 142–144.
[9] J. Yin, G.Y. Yuan, Z.H. Chu, J. Zhang, W.J. Ding, J. Mater. Res. 24 (2009) 3603–3610.
[10] J.Q. Li, L. Wang, H.W. Cheng, H.F. Zhang, Z.Q. Hu, H.N. Cai, J. Alloys Compd. 478 (2009) 827–830.
[11] E.S. Park, J.S. Kyeong, D.H. Kim, Mater. Sci. Eng. A 449–451 (2007) 225–229.
[12] J. Yin, G.Y. Yuan, P.F. Wang, J. Zhang, Z.H. Chu, W.J. Ding, J. Alloys Compd. 481 (2009) 407–410.
[13] C. Xia, L. Xing, W.Y. Long, Z.Y. Li, Y. Li, J. Alloys Compd. 484 (2009) 698–701.
[14] J.T. Zhang, W.M. Wang, H.J. Ma, G.H. Li, R. Li, Z.H. Zhang, Thermochim. Acta 505 (2010) 41–46.
[15] W.K. An, A.H. Cai, J.H. Li, Y. Luo, T.L. Li, X. Xiong, Y. Liu, Y. Pan, J. Non-Cryst. Solids 355 (2009) 1703–1706.
[16] A.H. Cai, W.K. An, Y. Luo, T.L. Li, X.S. Li, X. Xiong, Y. Liu, J. Alloys Compd. 490 (2010) 642–646.
[17] S.B. Qiu, K.F. Yao, J. Alloys Compd. 475 (2009) L5–L8.
[18] L. Liu, X.J. Zhao, C.L. Ma, T. Zhang, Intermetallics 17 (2009) 241–245.
[19] Y.T. Cheng, T.H. Hung, J.C. Huang, P.J. Hsieh, J.S.C. Jang, Mater. Sci. Eng. A 449–451 (2007) 501–505.
[20] L.J. Chang, J.S.C. Jang, B.C. Yang, J.C. Huang, J. Alloys Compd. 434–435 (2007) 221–224.
[21] L.J. Huang, L. Li, G.Y. Liang, Y.L. Guo, D.C. Wu, J. Non-Cryst. Solids 354 (2008) 1048–1053.
[22] H.C. Kou, J. Wang, H. Chang, B. Tang, J.S. Li, R. Hu, L. Zhou, J. Non-Cryst. Solids 355 (2009) 420–424.
[23] N. Bayri, T. Izgi, H. Gencer, P. Sovak, M. Gunes, S. Atalay, J. Non-Cryst. Solids 355 (2009) 12–16.
[24] M. Stoica, S. Kumar, S. Roth, S. Ram, J. Eckert, G. Vaughan, A.R. Yavari, J. Alloys Compd. 483 (2009) 632–637.
[25] S.H. Al-Heniti, J. Alloys Compd. 484 (2009) 177–184.
[26] A. Takeuchi, A. Inoue, Mater. Trans. JIM 46 (2005) 2817–2829.
[27] R. Bushch, Y.J. Kim, W.L. Johnson, J. Appl. Phys. 77 (1995) 4039–4043.

[28] X. Ou, G.Q. Zhang, X. Xu, L.N. Wang, J.F. Liu, J.Z. Jiang, J. Alloys Compd. 441 (2007) 181–184.
[29] H.E. Kissinger, Anal. Chem. 29 (1957) 1702–1706.
[30] H.R. Wang, Y.L. Gao, G.H. Min, X.D. Hui, Y.F. Ye, Phys. Lett. A 314 (2003) 81–87.
[31] F.X. Qin, H.F. Zhang, B.Z. Ding, Z.Q. Hu, Intermetallics 12 (2004) 1197–1203.
[32] L.C. Chen, F. Spaepen, Nature 336 (1988) 366–368.
[33] W.A. Johnson, R.F. Mehl, Trans. Am. Inst. Min. Metall. Pet. Eng 135 (1939) 416–422.
[34] M. Avrami, J. Chem. Phys. 7 (1939) 1103–1112.
[35] M. Avrami, J. Chem. Phys. 8 (1940) 212–224.
[36] M. Avrami, J. Chem. Phys. 9 (1941) 177–184.
[37] J.W. Christian, The Theory of Transformation in Metals and Alloys, 1st ed., Pergamon, Oxford, 1965.